Available online at www.sciencedirect.com
ScienceDirect
Journal of Membrane Science 310 (2008) 303–311
journal of MEMBRANE SCIENCE
www.elsevier.com/locate/memsci

Sulfonated poly(arylene thioether phosphine oxide)s copolymers for proton exchange membrane fuel cells

Xuhui Ma, Liping Shen, Chunjie Zhang, Guyu Xiao *, Deyue Yan **, Guoming Sun

College of Chemistry and Chemical Engineering, Shanghai Jiao Tong University, 800 Dongchuan Road, Shanghai 200240, PR China

Received 7 August 2007; received in revised form 1 November 2007; accepted 5 November 2007

Abstract

High molecular weight sulfonated poly(arylene thioether phosphine oxide)s (sPATPO) with various sulfonation degrees were prepared directly by aromatic nucleophilic polycondensation of 4,4′-thiobisbenzenethiol with sulfonated bis(4-fluorophenyl) phenyl phosphine oxide and bis(4-fluorophenyl) phenyl phosphine oxide. sPATPO in the acid form with sulfonation degrees of 60–100% exhibits a glass transition temperature higher than 230 °C and a 5% weight loss temperature above 400 °C, indicating high thermal stability. sPATPO with a high sulfonation degree shows high proton conductivity and good resistance to swelling as well. For instance, sPATPO-70 displays the conductivity of 0.0783 S/cm and a swelling ratio of 11.6% at 90 °C. TEM micrographs showed that sPATPO membranes with a high sulfonation degree could form continuous ion channels, which are favorable for improving the proton conductivity but harmful to remaining the mechanical property. The membranes are expected to show good performances in fuel cell applications.

Keywords: Poly(arylene thioether phosphine oxide)s; Proton exchange membrane; Sulfonate

1. Introduction

Proton exchange membrane fuel cells (PEMFCs) convert chemical energy directly into electrical energy with high efficiency and low emission of pollutants, and are widely used as automotive and stationary power sources [1,2]. The membrane electrode assembly (MEA), including the proton exchange membrane (PEM), catalyst layer and gas diffusion layer, is the most important component of PEMFCs [3]. The PEM is the heart of the MEA, which conducts protons from the anode to the cathode, supports the catalyst, and prevents the fuel (hydrogen, methanol) from contacting with oxygen directly. Up to now, the perfluorinated Nafion membranes, developed by DuPont 40 years ago, are the most widely used commercial products due to their overall performances [4,5]. However, the drawbacks such as the difficulty of synthesis, the high cost, and the great loss of conductivity at high temperature limit their popularization [6,7]. Therefore, the exploration of PEM with good comprehensive properties became an attractive research field in the past decade.

The engineering thermoplastics such as poly(arylene ether sulfone)s, poly(arylene ether ketone)s, polyimides, and polybenzimidazoles are widely investigated due to good mechanical property, thermal property, and high chemical stability. Those merits provoked many researchers to employ those engineering thermoplastics as the matrix of PEM [8–12]. Generally, there are two routes to prepare the engineering material based PEM [3,13]. One of them is the post-modification of the existing polymers by sulfonation, the other is the direct polycondensation method with sulfonated monomers. The latter showed more advantages in comparison with the former. In the latter method, the sulfonated position could be controlled by designing the specific sulfonated

* Corresponding author. Tel.: +86 21 54742665.
** Corresponding author.
E-mail addresses: gyxiao@sjtu.edu.cn (G. Xiao), dyyan@sjtu.edu.cn (D. Yan).

0376-7388/$ – see front matter © 2007 Elsevier B.V. All rights reserved.
doi:10.1016/j.memsci.2007.11.003

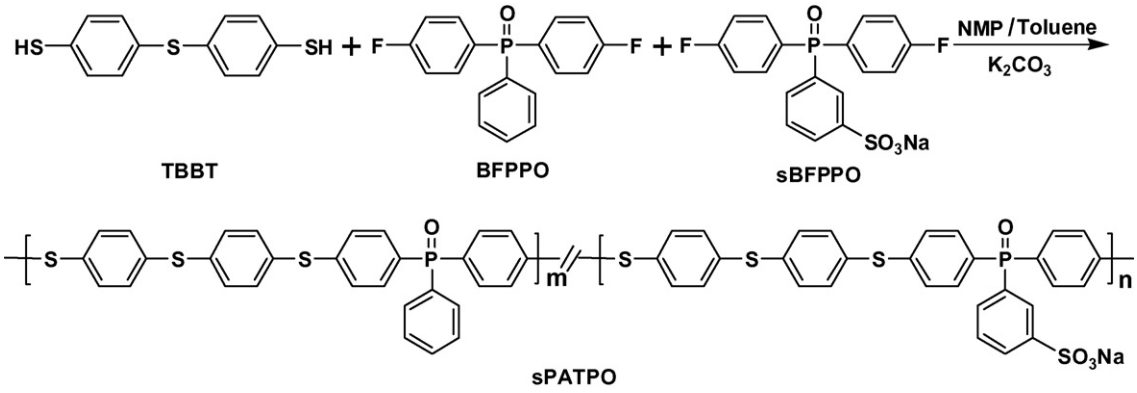

Scheme 1. Synthesis of PATPO and sPATPO.

monomer, and the sulfonation degree could be adjusted conveniently by changing the feed ratio of the sulfonated monomer to the non-sulfonated monomer. Furthermore, degradation and cross-linking were avoided.

Poly(arylene ether phosphine oxide)s and Poly(arylene thioether phosphine oxide)s show excellent mechanical property, thermal stability, and chemical stability [14,15]. Moreover, the phosphine oxide moieties endow materials with good water retention and adhesive ability with inorganic compounds. Therefore, they are of interest for fuel cell applications [16,17]. However, there appears to be little work reported on PEM materials derived from phosphine oxides. The group of McGrath reported the preparation of sulfonated poly(arylene ether phosphine oxide)s by direct polycondensation in a conference proceeding [18]. Our group prepared sulfonated poly(phthalazinone ether phosphine oxide)s via direct nucleophilic substitution polycondensation, showing excellent comprehensive property [19]. In this article, we report the synthesis of sulfonated poly(arylene thioether phosphine oxide)s (sPATPO) by direct polymerization of 4,4′-thiobisbenzenethiol with various ratios of sulfonated bis(4-fluorophenyl) phenyl phosphine oxide to bis(4-fluorophenyl) phenyl phosphine oxide. The performances of these membranes made from sPATPO are investigated in detail.

2. Experimental

2.1. Materials

Phenylphosphonic dichloride was purchased from Aldrich chemical Co. and used as received. 4,4′-thiobisbenzenethiol (TBBT) was purchased from Shou & Fu chemical Co., Ltd. and recrystallized from n-hexane prior to use. N-Methyl-2-Pyrrolidone (NMP) was purified by distillation under reduced pressure and stored over 4 Å molecular sieves. Tetrahydrofuran (THF) and toluene were dried with sodium and distilled before use. 4-Bromofluorobenzene, magnesium, fuming sulfonic acid and other reagents were obtained from commercial sources and used without further purification. Bis(4-fluorophenyl)phenyl phosphine oxide (BFPPO) was synthesized according to a previous report, and sulfonated bis(4-fluorophenyl)phenyl phosphine oxide (sBFPPO) was prepared by sulfonation of BFPPO according to a reported procedure [18,19].

2.2. Synthesis of polymers

Poly(arylene thioether phosphine oxide)s (PATPO) and a series of sulfonated poly (arylene thioether phosphine oxide)s (sPATPO-x) with different sulfonation degrees were prepared via the aromatic nucleophilic substitution polycondensation of TBBT with various feed ratios of sBFPPO to BFPPO in a NMP/toluene system, using K_2CO_3 as weak base to form the required thiophenolate nucleophile, where "*x*" represented the molar feed ratio of sBFPPO to BFPPO (Scheme 1). A typical procedure was showed as follows. 0.8764 g (0.0035 mol) of TBBT, 1.4571 g (0.0035 mol) of sBFPPO and 0.5321 g (0.00385 mol) of K_2CO_3 were added into a three-necked flask, equipped with a mechanical stirrer, a Dean-Stark trap with a condenser, and a nitrogen gas inlet/outlet. Dry NMP was introduced to obtain a 20% solid concentration and toluene was used as an azeotropic agent. The reaction mixture was heated to reflux at 160 °C (oil bath temperature) for 4 h to dehydrate the system. Then the reaction temperature was increased to 175 °C to distill the toluene. After removing the toluene thoroughly, the system was kept at 175 °C for 12 h and 190 °C for 48 h until the solution became very viscous. The black viscous mixture was cooled down 110 °C, then diluted with 2 ml of NMP and poured into 300 ml of de-ionized water with vigorous stirring to produce the fibrous polymer. The polymer was washed with boiling water for several times to remove the inorganic salts and dried under vacuum at 100 °C for 48 h.

Yield: 98%. ^{1}H NMR (DMSO-d_6, ppm): 7.92-7.86 (1H), 7.86–7.80 (1H), 7.60–7.46 (6H), 7.46–7.41 (4H), 7.40–7.30 (8H). ^{13}C NMR (DMSO-d_6, ppm): 153.888 (d, J_{CP} = 10.6 Hz), 146.908 (d, J_{CP} = 3.0 Hz), 140.477, 139.303, 137.700 (d, J_{CP} = 9.1 Hz), 137.277, 136.956 (d, J_{CP} = 10.7 Hz), 136.865, 136.515, 134.914 (d, J_{CP} = 103.7 Hz), 134.732, 133.909 (d, J_{CP} = 12.2 Hz), 133.595 (d, J_{CP} = 9.2 Hz), 133.519 (d, J_{CP} = 12.2 Hz).

2.3. Preparation of membranes

The ionomer in the salt form was completely dissolved in dimethyl sulfoxide (DMSO). Then the ionomer solution was

poured slowly onto a dust-free glass plate and dried at 65 °C for 3 days. The membranes were peeled off from the glass plate by immersing them in deionized water for several minutes. Thus the transparent and ductile membranes were obtained. The membranes in the salt form were converted into the corresponding membranes in the acid form by soaking them in 1 M HCl for 48 h.

3. Characterization and measurements

3.1. FT–IR

FT–IR spectra of the polymers were recorded on a Bruker Equinox-55 Fourier transform spectrometer.

3.2. NMR

NMR spectra were recorded on a Varian MERCURY plus 400 MHz spectrometer. Deuterated dimethyl sulfoxide (DMSO-d_6) was used as the solvent. Tetramethylsilane was used as the internal standard.

3.3. GPC measurements

The molecular weight and molecular weight distribution of the polymers were determined by a PE Series 200 gel permeation chromatography (GPC), equipped a mixed 5 μ PS columns (range of pore sizes: 1 × 105, 1 × 104, and 1 × 103 Å) and a refractive index detector. All samples were run in *N*,*N*-dimethylformamide (DMF) at room temperature with a flow rate of 1.0 ml/min. Polystyrene standards were used for calibration.

3.4. Thermal properties

3.4.1. Differential scanning calorimetry (DSC)

The glass transition temperature (T_g) of PATPO and sPATPO were obtained on a PE Pyris-1 differential scanning calorimeter (DSC). The samples in the acid form for DSC analysis were preheated under nitrogen protection at 150 °C for 30 min to remove moisture and then cooled down 80 °C. The DSC curves were recorded from 80 °C to 300 °C at 10 °C/min.

3.4.2. Thermogravimetric analysis (TGA)

The thermal stability of PATPO and sPATPO was conducted using a PE TGA-7 thermogravimetric analyzer (TGA). The samples in the acid form for TGA analysis were also preheated under a nitrogen flow at 150 °C for 30 min to remove moisture and then cooled down 90 °C. The TGA curves were performed from 90 °C to 800 °C at 20 °C/min.

3.5. Ion exchange capacity (IEC)

The titration method was used to determine the IEC. The membranes in the acid form were soaked in saturated NaCl solution for 3 days, to replace the H^+ with the Na^+ thoroughly. Then the free H^+ was titrated by 0.01 M NaOH solution using phenolphthalein as the indicator. The value of IEC was obtained by the following equation:

$$\text{IEC} = \frac{(N_{\text{NaOH}} \times V_{\text{NaOH}})}{W_{\text{dry}}} \times 100\%$$

where N_{NaOH}, V_{NaOH} and W_{dry} were the concentration, the consumed volume of NaOH solution and the weight of dry membranes, respectively.

3.6. Water uptake and swelling ratio

The membranes in the acid form were dried under vacuum at 120 °C for 24 h. Then the weight and the length of the dry membrane were obtained as the benchmark. The dry membrane was then soaked in de-ionized water at the designed temperatures for the same interval (24 h) to ensure the membrane was saturated with water. Thereafter, the membrane was taken out and water on the membrane surface was removed quickly with tissue paper. The wet membrane was weighed and its length was gauged immediately. The water uptake and swelling ratio of the samples were calculated by the following equations:

$$\text{water uptake} = \frac{(W_{\text{wet}} - W_{\text{dry}})}{W_{\text{dry}}} \times 100\%$$

$$\text{swelling ratio} = \frac{(L_{\text{wet}} - L_{\text{dry}})}{L_{\text{dry}}} \times 100\%$$

where W_{wet} and W_{dry} were the mass of the wet and dry membrane, L_{wet} and L_{dry} were the length of the wet and dry membrane, respectively.

3.7. Proton conductivity

Proton conductivity measurements were run according to a previous report by a solatron 1260 gain phase analyzer over a frequency range from 10^7 Hz to 0.1 Hz [20]. The samples (20 mm × 8 mm) were washed three times with ultrapure water, then submersed in ultrapure water for 48 h before measurement. The sample was clamped by the mould. Thereafter, the mould was placed in a vessel, filled with ultrapure water at the designed temperatures. The conductivity (σ) of the sample in the longitudinal direction was calculated by the formula $\sigma = L/(RA)$, where L, A, and R were the distance between the two electrodes, the cross-sectional area of the membrane, and the membrane resistance, respectively.

3.8. Microstructure of membranes

The preparation procedure of the samples for transmission electron microscopy (TEM) investigation is similar to the previous report [21]. The membranes in the salt form were soaked in 1 M $AgNO_3$ solution for 12 h, and the used $AgNO_3$ solution was replaced with the fresh $AgNO_3$ solution (1 M), the above process was repeated three times. After the procedure, the membranes in the Na^+ form were completely convert into the corresponding Ag^+ form. Thereafter, they were immersed in de-ionized water

Table 1
Preparation results of polymers

Polymers	sBFPPO/BFPPO (molar ratio)	GPC			Yield (%)
		$M_n \times 10^3$	$M_w \times 10^3$	PDI	
PATPO	0/100	–[a]	–[a]	–[a]	96
sPATPO-60	60/40	77.8	128.4	1.65	96
sPATPO-70	70/30	79.6	115.8	1.45	97
sPATPO-80	80/20	86.0	135.8	1.60	97
sPATPO-90	90/10	94.5	155.6	1.65	97
sPATPO-100	100/0	115.3	199.4	1.73	98

[a] Poor solubility of PATPO in DMF.

for 12 h in order to remove the $AgNO_3$ solution on the membrane's surface. The membranes in the Ag^+ form were dried under vacuum and dissolved in DMSO. The solution was filtered and cast directly onto the copper grid for TEM investigation. The TEM images were determined using JEOL JSM-2010.

4. Results and discussion

4.1. Preparation of polymers

The conventional aromatic nucleophilic substitution polymerization was adopted to synthesize PATPO and sPATPO (Scheme 1). It is well-known that the fluorine atom of the deactivated aromatic rings is a good leaving group, promoting the nucleophilic substitution reaction. The –SH group reacted with the weak base (K_2CO_3) to form the $–S^-$ anion, and it attacked the aromatic carbon connected with the fluorine atom to turn into the aromatic thioether groups and thus produce the resulting polymers, due to its high nucleophilicity [22]. The sulfonated resultants all have high molecular weights, higher than 70,000 g/mol. Table 1 also indicates that the molecular weight of the resulting polymers increases with an increase of sulfonation degrees, which demonstrates that the sulfonated monomer sBFPPO enhanced the reactivity of the polycondensation. The reason is that the strong electron-withdrawing $–SO_3Na$ group endows the aromatic carbon atom, connected with fluorine atom, with high positive charges. It also could be found in Table 1 that the polydispersity index (PDI) is in a range from 1.45 to 1.73.

The ^1H NMR spectrum of sPATPO-100 is shown in Fig. 1(a). The hydrogen atoms of sPATPO-100, such as Hydrogen atom "2", "3", "6", "11", and "12", are separated and could be assigned, the splitting of them is clear. However, Hydrogen atom "7", "10", and "14" overlap seriously and the splitting of them is difficult to be determined. The ^{13}C NMR and dept spectra of sPATPO-100 are displayed in Fig. 1(b). The peak of Carbon atom "11" overlapped heavily with that of Carbon atom "6". The local amplifying picture, containing the peaks of Carbon atom "6", "11" and "14", is inserted into Fig. 1(b) in order to read the peak of Carbon atom "11" clearly. Carbon atom "8" showed two low splitting peaks with the coupling constant J_{CP} of 103.7 Hz, while Carbon atom "9" showed only a very low peak at 136.865 ppm and no splitting peaks. Similar to Carbon atom "8", Carbon atom "9" should indicate two splitting peaks with the coupling constant close to that of Carbon atom "8" (J_{CP} = 103.7 Hz), located

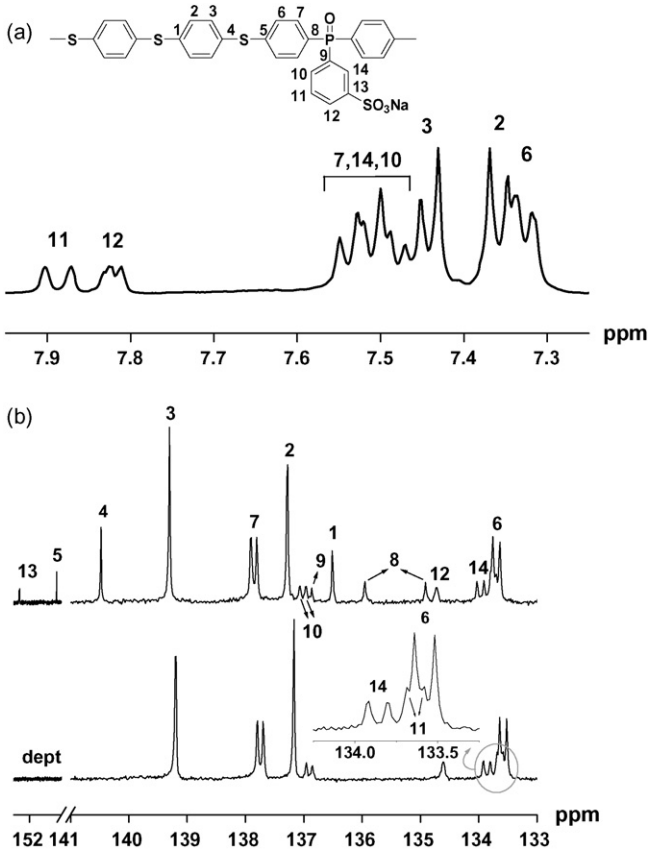

Fig. 1. (a) ^1H NMR spectrum of sPATPO-100; (b) ^{13}C NMR spectra of sPATPO-100.

at about 137.9 ppm. Unfortunately, the strong splitting peaks of Carbon atom "7" were at around 138.0–137.7 ppm, which might shield one of the very low splitting peak of Carbon atom "9", leading to its disappearance.

The successful introduction of $–SO_3Na$ groups is also confirmed by comparing the IR spectrum of PATPO with that of sPATPO (Fig. 2). The absorption band at 1198 cm^{-1} is ascribed to the characteristic peak of triphenyl phosphine oxide, which appeared in the spectra of both PATPO and sPATPO. However, the absorption bands at 1108 and 1036 cm^{-1} are only presented

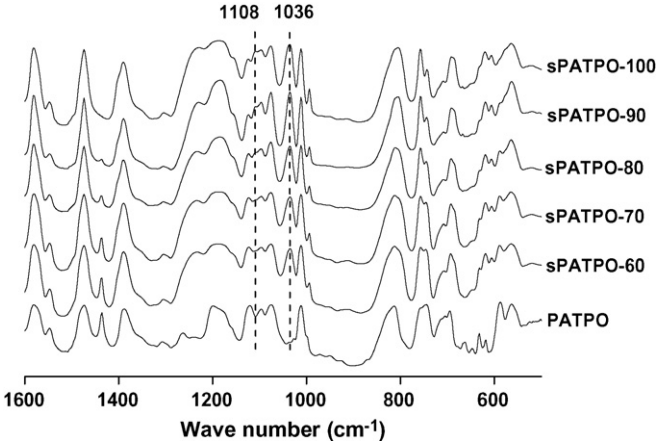

Fig. 2. IR spectra of PATPO and sPATPO.

Table 2
Properties of polymers

Polymers	T_g (°C)	T_{d5} (°C)	IEC(meq/g)	
			Calc.[a]	Meas.[b]
PATPO	181	500	–	–
sPATPO-60	235	421	1.03	0.99
sPATPO-70	241	420	1.18	1.14
sPATPO-80	245	412	1.32	1.28
sPATPO-90	249	408	1.46	1.42
sPATPO-100	252	405	1.60	1.56

[a] The calculated IEC.
[b] The measured IEC.

in the spectra of sPATPO, which are assigned to the asymmetric and symmetric stretching vibrations of sodium sulfonate groups, respectively. In addition, the characteristic peak intensity of sodium sulfonate groups increases with increasing feed ratios of sBFPPO to BFPPO, suggesting that the $–SO_3Na$ groups were incorporated into the polymer backbone quantitatively.

4.2. Thermal analysis of polymers

4.2.1. DSC

The DSC thermograms of PATPO and sPATPO in the acid form are shown in Fig. 3(a) and their T_g are listed in Table 2. All the polymers indicated glass transitions though it was not distinct for some of them. They displayed high glass transition temperatures. PATPO showed the T_g of 181 °C, while sPATPO showed the T_g in the range of 235–252 °C, much higher than that of PATPO. Furthermore, the T_g of the samples increased with increasing sulfonation degrees, ranging from 181 °C for PATPO to 252 °C for sPATPO-100, similar to the previous reports [10,23]. T_g reflects the mobility of polymer chains. The effects of pendant sulfonic acid groups on the mobility of molecule segments include two aspects. The pendant sulfonic acid groups associate and enhance the intermolecular interaction. On the other hand, the pendant sulfonic acid groups are large and bulky. Both the associative effect and the bulkiness of the sulfonic acid groups hinder the mobility of molecule segments. Therefore, the pendant sulfonic acid groups increased the T_g of the products, and the more feed ratio of sBFPPO to BFPPO, the higher the T_g of the products.

4.2.2. TGA

The TGA curves of PATPO and sPATPO in the acid form are displayed in Fig. 3(b) and the 5% mass loss temperature (T_{d5}) of the polymers is listed in Table 2. Fig. 3(b) shows that the homopolymer PATPO had only one clear weight loss step which appears at ~500 °C, ascribed to the polymer backbone degradation. However, the weight loss of sulfonated polymers (sPATPO) includes two sequential degradation steps. The first step is distinct, around at 400 °C, which is attributed to the desulfonation process. Conversely, the second one is somewhat indistinct. It appeared approximately at 450 °C, due to the degradation of the polymer main chain. It can be read from Table 2 that the T_{d5} of PATPO is 500 °C, and that the T_{d5} of sPATPO is in the range of 405–421 °C. Similar to the reported studies, the T_{d5} decreased slightly with the increase of the sulfonation degree due to desulfonation [24,25]. sPATPOs show high thermal stability for fuel cell applications.

The sulfonic acid groups of sPATPO were located in the pendant phenyl rings. The T_{d5} of them is higher than that of sulfonated poly(arylene ether)s with an equal IEC, bearing sulfonic acid groups in the backbone, showing better thermal stability when compared to sulfonated poly(arylene ether)s with sulfonic acid groups in the mainchain [24,25].

4.3. IEC

The IEC of the membranes is determined by the titration method and compiled in Table 2. As expected, the IEC values increased linearly with increasing the sulfonation degree. Moreover, the measured IEC was in good consistent with the calculated one, indicating further that the monomer sBFPPO was successfully incorporated into the polymer backbone without side reactions, which was often observed in the post-sulfonation strategy.

4.4. Water uptake and swelling ratio

PEM such as sulfonated poly(arylene ether)s showed a hydrophilic/hydrophobic nano-separation morphology. The hydrophobic domain provided the mechanical stability, whereas the hydrated hydrophilic part was responsible for the proton

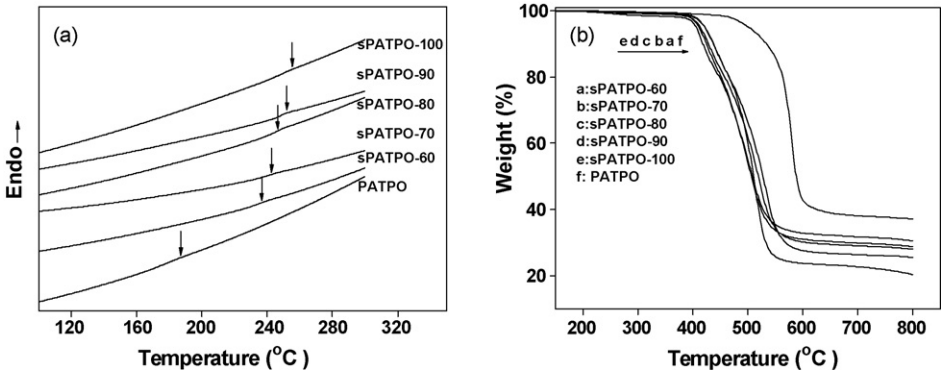

Fig. 3. (a) DSC curves of PATPO and sPATPO; (b) TGA curves of PATPO and sPATPO.

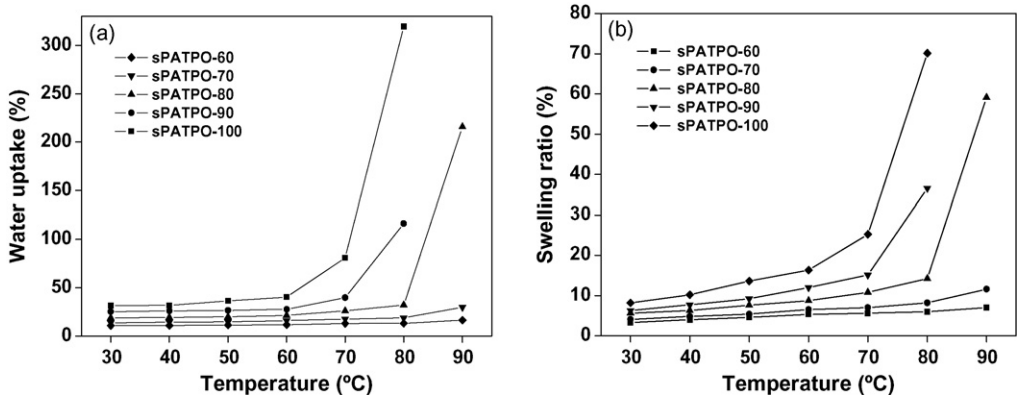

Fig. 4. (a) Water uptake of sPATPO at various temperatures; (b) Swelling ratio of sPATPO at various temperatures.

conductivity [6]. The water content of proton exchange membranes has a great effect on the membrane's proton conductivity and mechanical properties. An appropriate amount of water content is necessary for a PEM so as to conduct the hydrated proton from the anode to the cathode, but excessive water content leads to a further phase separation or too much swelling, thus losing the mechanical properties. In order to obtain the balance between the proton conductivity and mechanical properties, the water uptake of membrane materials is of importance. The water uptake and swelling ratio of the membranes as a function of temperatures and sulfonation degrees are plotted in Fig. 4. Fig. 4(a) shows that the water uptake of the membrane increases with increasing both the temperature and sulfonation degree. Under 60 °C, the water uptake increases a little bit no matter whether the sulfonation degree of membranes is high or low. The water uptake of sPATPO-60 and -70 increases very slowly within the whole testing temperature range due to their low sulfonation degrees. For example, sPATPO-70 exhibits the water uptake of 19% at 80 °C compared with 30% for Nafion 117 [26]. The water uptake of sPATPO-80 enhances slowly when the temperature is less than 80 °C and then enhances suddenly, reaching 215.8% at 90 °C. The water uptake of sPATPO-90 and -100 elevates moderately in the range of 30–70 °C and then elevates abruptly, reaching 116.2% and 319.4% at 80 °C, respectively, which are much higher than that of Nafion 117. Furthermore, sPATPO-90 and -100, with a high sulfonation degree, become soluble after 24 h water exposure at 90 °C.

The swelling ratio as a function of the temperature and sulfonation degree is displayed in Fig. 4(b). The swelling ratio curves are very similar to the water uptake curves. At low temperature (≤70 °C), the swelling ratio of all the membranes increase slowly. Thereafter, the membranes with lower sulfonation degrees such as sPATPO-60 and -70 still exhibit very low increase in swelling in the range of RT ~ 90 °C, reaching 7% and 11.6% at 80 °C compared with 20% for Nafion 117 [25]. The swelling ratio of sPATPO-80 also enhances slowly up to 80 °C, then enhances drastically and reaches 59.1% at 90 °C. The swelling ratio of sPATPO-90 and -100 elevates rapidly, reaching 36.6% and 70.1% at 80 °C, respectively. sPATPO-90 and -100 dissolved in water at 90 °C and thus lost their mechanical integrity.

4.5. Proton conductivity

In order to be fully hydrated before the measurements, all membranes in the acid form were immersed in ultrapure water at room temperature for 48 h. The proton conductivity of sPATPO as a function of temperatures is shown in Fig. 5. As expected, the proton conductivity increases with increasing the temperature and sulfonation degree. The proton conductivity of sPATPO-60 increases very slowly due to its low IEC, reaching 1.16×10^{-2} S/cm even at 90 °C. For sPATPO-70 and -80, their proton conductivity enhances slowly when the temperature is less than 60 °C, but enhances obviously over 70 °C and reach 7.83×10^{-2} and 9.65×10^{-2} S/cm at 90 °C, respectively. Similarly, for sPATPO-90 and -100 with high sulfonation degrees, their proton conductivity increases obviously with increasing temperatures, which reaches 9.54×10^{-2} and 12.0×10^{-2} S/cm at 80 °C, close to or higher than that (9.6×10^{-2} S/cm) of Nafion 117 [25]. The proton conductivity values of these two membranes at 90 °C could not be obtained because they dissolved in water at this temperature.

sPATPO-80, -90 and -100 show a sharp increase in the water uptake at high temperatures, while they only indicate a gradual increase in the conductivity. In a definite range of the water uptake, their conductivity enhances greatly with the increasing water uptake, the absorbed water improves the proton conduc-

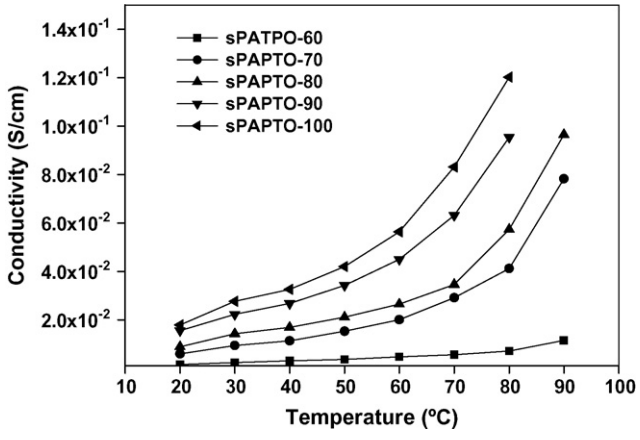

Fig. 5. Conductivity of sPATPO at various temperatures.

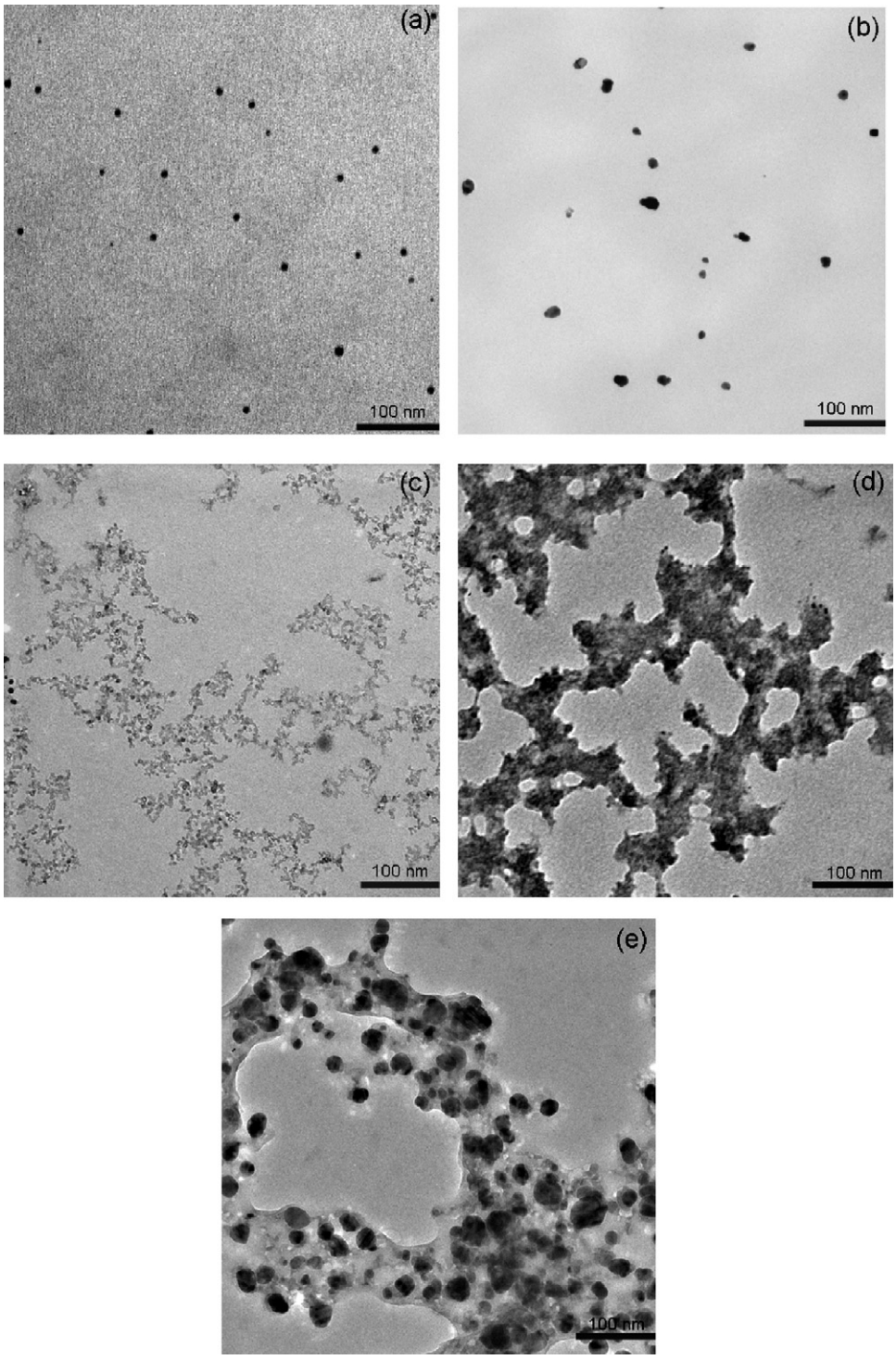

Fig. 6. TEM micrographs of sPATPO membranes (a) sPATPO-60, (b) sPATPO-70, (c) sPATPO-80, (d) sPATPO-90, (e) sPATPO-100.

tion. But above this range, their conductivity increases slowly. As the literature reported, when the water uptake of PEM is too much high, the absorbed water serves to dilute the proton concentration, this factor negatively affects the conductivity of PEM [27]. Both the above positive and negative effects of the absorbed water on the conductivity render the values of the conductivity increase slowly. For some PEM, their conductivity even decreases with increasing the water uptake if the negative effect of the absorbed water on the conductivity surpasses its positive effect on the conductivity [27].

Although sPATPO-90 and -100 showed excellent proton conductivity at 80 °C, the excessive swelling limits their application in fuel cells. On the contrary, sPATPO-70 showed not only a high proton conductivity but also a reasonable swelling ratio, so they could be considered as the promising candidates in PEM application.

4.6. Microstructure of membranes

The macroscopic properties of membranes, such as the water uptake, swelling ratio, and proton conductivity, are strongly related to their microstructure. The previous studies have demonstrated that sulfonic acid groups can chelate with heavy metal ions such as Ag^+ and Pb^+ to improve the contrast of the micrograph [28–31]. Therefore, sPATPO membrane samples used for transmission electron microscopy were transformed into the Ag^+ salt form, TEM micrographs are shown in Fig. 6. The copolymers exhibit the nanophase morphology as indicated by the dark and light regions, which was similar to other ionomers [6]. The dark regions in the image represent localized ionic domains while the light regions stand for the hydrophobic aromatic segments. Fig. 6 displays that the sulfonation degree of sPATPO affects their microstructure greatly. For the samples sPATPO-60 and -70 with low sulfonation degrees, the spherical silver particles are randomly dispersed in the polymer matrix with the approximate sizes of 8 and 15 nm, respectively. This distribution of sulfonic acid groups in the ionomers is dispersive, not connective, resulting in the low swelling ratio and proton conductivity. However, with increasing the sulfonation degree, the silver particles in the matrix of ionomers aggregate into bigger and bigger, forming the continuous hydrophilic ion channel network. For sPATPO-80, the hydrophilic network is connective, the channel width of which is about 7 nm (Fig. 5c), whereas the hydrophilic network of sPATPO-90 and -100 is perforative, forming the hydrophilic channel of 50 and 140 nm width, respectively. The hydrophilic ion channels absorb water and conduct the proton while the hydrophobic domains provide mechanical strength. The ion domains become big and even turn into continuous channels with increasing the sulfonation degree, which lead to the high proton conductivity and low strength. Particularly, sPATPO-90 and -100 dissolved in water at 90 °C and lost their strength because of their excessive swelling after hot water exposure.

5. Conclusions

High molecular weight poly(arylene thioether phosphine oxide) (PATPO) and a series of sulfonated poly(arylene thioether phosphine oxide)s (sPATPO) with various sulfonation degrees were prepared by direct polycondensation. The structure of the resulting polymers was confirmed by IR and NMR. The ductile and tough membranes in the salt form were obtained conveniently by solvent casting from DMSO solution. DSC and TGA showed that the acid form ionomers exhibited high glass transition temperature and high thermal stability. TEM micrographs showed that sPATPO membranes with high sulfonation degree, such as sPATPO-80, -90 and -100, can form continuous ion channels, which are favorable for improving the proton conductivity but harmful to remaining the mechanical property. sPATPO-70 showed not only a high proton conductivity but also a reasonable swelling ratio, indicating that it was the promising membrane for fuel cells.

Acknowledgements

The authors thank the National Natural Science Foundation of China (No. 50303010), the Special Funds for Major State Basic Research Projects (2005CB623803), the National High Technical Research Development Program (No. 2002AA323040), and the Science and Technology Committee of Shanghai municipality (No. 065207065 and No. 07DJ14004) for their support of this research.

References

[1] M.A. Hickner, H. Ghassemi, Y.S. Kim, B.R. Einsla, J.E. McGrath, Alternative polymer systems for proton exchange membranes (PEMs), Chem. Rev. 104 (2004) 4587–4612.
[2] A. Colliera, H. Wang, X. Yuan, J. Zhang, D.P. Wilkinsona, Degradation of polymer electrolyte membranes, Int. J. Hydrogen Energ. 31 (2006) 1838–1854.
[3] Z.W. Bai, M.F. Durstock, T.D. Dang, Proton conductivity and properties of sulfonated polyarylenethioether sulfones as proton exchange membranes in fuel cells, J. Membr. Sci. 281 (2006) 508–516.
[4] Q.F. Li, R.H. He, J.O. Jensen, N.J. Bjerrum, Approaches and recent development of polymer electrolyte membranes for fuel cells operating above 100 °C, Chem. Mater. 15 (2003) 4896–4915.
[5] O. Savadogo, Emerging membranes for electrochemical systems: (I) solid polymer electrolyte membranes for fuel cell systems, J. New Mat. Electrochem. Syst. 1 (1998) 47–66.
[6] K.D. Kreuer, On the development of proton conducting polymer membranes for hydrogen and methanol fuel cells, J. Membr. Sci. 185 (2001) 29–39.
[7] S. Swier, V. Ramani, J.M. Fenton, H.R. Kunz, M.T. Shaw, R.A. Weiss, Polymer blends based on sulfonated poly(ether ketone ketone) and poly(ether sulfone) as proton exchange membranes for fuel cells, J. Membr. Sci. 256 (2005) 122–133.
[8] K. Miyatake, Y. Chikashige, M. Watanabe, Novel sulfonated poly(arylene ether): a proton conductive polymer electrolyte designed for fuel cells, Macromolecules 36 (2003) 9691–9693.
[9] X.C. Ge, Y. Xu, M. Xiao, Y.Z. Meng, A.S. Hay, Synthesis and characterization of poly(arylene ether)s containing triphenylmethane moieties for proton exchange membrane, Eur. Polym. J. 42 (2006) 1206–1214.
[10] P.X. Xing, G.P. Robertson, M.D. Guiver, S.D. Mikhailenko, K.P. Wang, K. Serge, Synthesis and characterization of sulfonated poly(ether ether ketone) for proton exchange membranes, J. Membr. Sci. 229 (2004) 95–106.
[11] B.R. Einsla, Y.T. Hong, Y.S. Kim, F. Wang, N.Z. Gunduz, J.E. McGrath, Sulfonated naphthalene dianhydride based polyimide copolymers for proton-exchange-membrane fuel cells. I. Monomer and copolymer synthesis, J. Polym. Sci. A: Polym. Chem. 42 (2004) 862–874.
[12] D.J. Jones, J. Rozière, Recent advances in the functionalisation of polybenzimidazole and polyetherketone for fuel cell applications, J. Membr. Sci. 185 (2001) 41–58.
[13] S.M.J. Zaidi, S.D. Mikhailenko, G.P. Robertson, M.D. Guiver, S. Kaliaguine, Proton conducting composite membranes from poly(ether ether ketone) and heteropolyacids for fuel cell applications, J. Membr. Sci. 173 (2000) 17–34.
[14] C.D. Smith, A. Gungor, K.M. Keister, H.A. Marand, J.E. McGrath, Poly(arylene ether ketone)-poly(arylene ether phosphine oxide) copolymer and blend compositions, Polym. Prepr. 32 (1991) 93–95.
[15] S. Wang, H. Zhuang, H.K. Shobha, T.E. Glass, M. Sankarapandian, Q. Ji, A.R. Shultz, J.E. McGrath, Miscibility of poly(arylene phosphine oxide) systems and bisphenol a poly(hydroxy ether), Macromolecules 34 (2001) 8051–8063.
[16] D.J. Riley, A. Gungor, S.A. Srinivason, M. Sankarapandian, C.N. Tchatchoua, M.W. Muggli, T.C. Ward, J.E. McGrath, Synthesis and characterization of flame resistant poly(arylene ether)s, Polym. Eng. Sci. 37 (1997) 1501–1511.

[17] S. Wang, Q. Ji, C.N. Tchatchoua, A.R. Shultz, J.E. Mcgrath, Phosphonyl/hydroxyl hydrogen bonding-induced miscibility of poly(arylene ether phosphine oxide/sulfone) statistical copolymers with poly(hydroxy ether) (phenoxy resin): synthesis and characterization, J. Polym. Sci. B: Polym. Phys. 37 (1999) 1849–1862.
[18] H.K. Shobha, G.R. Smalley, M. Sankarapandian, J.E. McGrath, Synthesis and characterization of sulfonated poly(arylene ether)s based on functionalized triphenyl phosphine oxide for proton exchange membranes, Polym. Prepr. 41 (2000) 180–181.
[19] X. Ma, C. Zhang, G. Xiao, D. Yan, G. Sun, Synthesis of Sulfonated poly(phthalazinone ether phosphine oxide)s by direct polycondensation for proton exchange membranes, J. Polym. Sci. A: Polym. Chem. in press.
[20] X.F. Li, C.J. Zhao, H. Liu, Z. Wang, H. Na, Direct synthesis of sulfonated poly(ether ether ketone ketone)s (SPEEKKs) proton exchange membranes for fuel cell application, Polymer 46 (2005) 5820–5827.
[21] X.F. Li, C.P. Liu, H. Lu, C.J. Zhao, Z. Wang, W. Xing, H. Na, Preparation and characterization of sulfonated poly(ether ether ketoneketone) proton exchange membranes for fuel cell application, J. Membr. Sci. 255 (2005) 149–155.
[22] H.K. Shobha, M. Sankarapandian, T.E. Glass, J.E. McGrath, Sulfonated aromatic diamines as precursors for polyimides for proton exchange membranes, Polym. Prepr. 41 (2000) 1298–1299.
[23] S. Gu, G.H. He, X.M. Wu, C.N. Li, H.J. Liu, C. Lin, X.G. Li, Synthesis and characteristics of sulfonated poly(phthalazinone ether sulfone ketone) (SPPESK) for direct methanol fuel cell (DMFC), J. Membr. Sci. 281 (2006) 121–129.
[24] F. Wang, M. Hickner, Y.S. Kim, T.A. Zawodzinski, J.E. McGrath, Direct polymerization of sulfonated poly(arylene ether sulfone) random (statistical) copolymers: Candidates for new proton exchange membranes, J. Membr. Sci. 197 (2002) 231–242.
[25] Y. Gao, G.P. Robertson, M.D. Guiver, S.D. Mikhailenko, X. Li, S. Kaliaguine, Low-swelling proton-conducting copoly(aryl ether nitrile)s containing naphthalene structure with sulfonic acid groups meta to the ether linkage, Polymer 47 (2006) 808–816.
[26] P.X. Xing, G.P. Robertson, M.D. Guiver, S.D. Mikhailenko, S. Kaliaguine, Sulfonated Poly(aryl ether ketone)s Containing the Hexafluoroisopropylidene Diphenyl Moiety Prepared by Direct Copolymerization, as Proton Exchange Membranes for Fuel Cell Application, Macromolecules 37 (2004) 7960–7967.
[27] Z.Q. Shi, S. Holdcroft, Synthesis and proton conductivity of partially sulfonated poly([vinylidene difluoride-co-hexafluoropropylene]-b-styrene) block copolymers, Macromolecules 38 (2005) 4193–4201.
[28] K. Miyatake, Y. Chikashige, E. Higuchi, M. Watanabe, Tuned polymer electrolyte membranes based on aromatic polyethers for fuel cell applications, J. Am. Chem. Soc. 129 (2007) 3879–3887.
[29] M.A. Hickner, C.H. Fujimoto, C.J. Cornelius, Transport in sulfonated poly(phenylene)s: Proton conductivity, permeability, and the state of water, Polymer 47 (2006) 4238–4244.
[30] M. Gil, X.L. Ji, X.F. Li, H. Na, J.E. Hampsey, Y.F. Lu, Direct synthesis of sulfonated aromatic poly(ether ether ketone) proton exchange membranes for fuel cell applications, J. Membr. Sci. 234 (2004) 75–81.
[31] S.Q. Wu, Z.M. Qiu, S.B. Zhang, X.R. Yang, F. Yang, Z.Y. Li, The direct synthesis of wholly aromatic poly(p-phenylene)s bearing sulfobenzoyl side groups as proton exchange membranes, Polymer 47 (2006) 6993–7000.